Experimental and Molecular Pathology 134 (2023) 104874

Contents lists available at ScienceDirect

Experimental and Molecular Pathology

journal homepage: www.elsevier.com/locate/yexmp

SARS-CoV-2 hampers dopamine production in iPSC-derived dopaminergic neurons

G. Cappelletti [a,1], E.V. Carsana [b,1], G. Lunghi [b,1], S. Breviario [b], C. Vanetti [a], A.B. Di Fonzo [d], E. Frattini [d], M. Magni [d], S. Zecchini [a], M. Clerici [c,e], M. Aureli [b,2], C. Fenizia [c,2,*]

[a] Department of Biomedical and Clinical Sciences, University of Milan, via G.B. Grassi 74, 20157 Milan, Italy
[b] Department of Medical Biotechnologies and Translational Medicine, University of Milan, via F.lli Cervi 93, 20054 Segrate, Italy
[c] Department of Pathophysiology and Transplantation, University of Milan, via F. Sforza 35, 20122 Milan, Italy
[d] IRCCS Foundation Ca' Granda Ospedale Maggiore Policlinico, Dino Ferrari Center, Neuroscience Section, Department of Pathophysiology and Transplantation, University of Milan, via F. Sforza 35, 20122 Milan, Italy
[e] IRCCS Fondazione Don Gnocchi, via Capecelatro 66, 20148 Milan, Italy

ARTICLE INFO

Keywords:
SARS-CoV-2 infection
Dopaminergic neurons
Post COVID
Dopamine
Neuronal stress
SARS-CoV-2 variants

ABSTRACT

An increasing number of patients experiences prolonged symptoms, whose profile and timeline remain uncertain, a condition that has been defined as post COVID. The majority of recovered hospitalized patients manifests at least one persistent symptom even sixty days after the first clinical manifestation's onset. Particularly, in light of the COVID-19-related symptomatology, it has been hypothesized that SARS-CoV-2 might affect the dopamine pathway. However, no scientific evidence has been produced so far.

To this end, human iPSC-derived dopaminergic neurons were infected with EU, Delta and Omicron SARS-CoV-2 variants. The infection with EU and Delta variants, but not with Omicron, results in a reduced intracellular content and extracellular release of dopamine. Indeed, the tyrosine hydroxylase was found to be significantly upregulated at the mRNA level, while being greatly reduced at the protein level. The major downstream synthetic enzyme DOPA-decarboxylase and the dopamine transporter were significantly downregulated both at the mRNA and protein level. Notably, *in vitro* SARS-CoV-2 infection was also associated with an altered MAP2 and TAU expression and with an increased presence of neuronal stress markers.

These preliminary observations suggest that the dopamine metabolism and production are affected by SARS-CoV-2, partially explaining some of the neurological symptoms manifested.

1. Introduction

After two years of SARS-CoV-2 pandemic, a number of scientific and medical successes have been achieved, including the ongoing vaccine campaign. So far, the aim has been legitimately centered on the containment of COVID-19 severe or fatal illness. However, recent studies show that an increasing number of patients, even with an initial favorable COVID-19 outcome, experiences prolonged symptoms, whose profile and timeline is uncertain (CDC. Centers for Disease Control and Prevention, 2020). Such collection of symptoms, which develops during or following SARS-CoV-2 infection and which continues for >12 weeks, is currently named Long COVID or Post-COVID condition (Davis et al., 2021; CDC. Centers for Disease Control and Prevention, 2022; Soriano et al., 2022). It was reported that the majority of recovered hospitalized patients (>80%) presents at least one persistent symptom sixty days after symptomatology's onset, which commonly involves fatigue and dyspnea (Carfì et al., 2020). Moreover, after six months, beyond 30% of the patients displays other prolonged symptoms such as post exertional malaise, brain fog, neurological sensations, headaches, memory issues, insomnia, muscles aches, dizziness and balance issues, speech issues, joint pain, sleep disturbance, anxiety and depression (Davis et al., 2021; Huang et al., 2021; Tomasoni et al., 2021).

Since the beginning of the current pandemic, it has been evident that SARS-CoV-2 is able to penetrate and affect the nervous system, as

* Corresponding author at: Department of Pathophysiology and Transplantation, University of Milan, via F. Sforza 35, 20122 Milan, Italy.
E-mail address: claudio.fenizia@unimi.it (C. Fenizia).
[1] Equally contributed.
[2] Equally contributed.

https://doi.org/10.1016/j.yexmp.2023.104874
Received 8 May 2023; Received in revised form 14 September 2023; Accepted 26 September 2023

demonstrated by the plethora of neurological complications in infected patients. Such signs span from the highly frequent anosmia or ageusia (26%) to headache (37%) and encephalitis (0.5%) (Wan et al., 2021; Chou et al., 2021). Recently, it has been reported that SARS-CoV-2 infection has a direct impact on the brain. Indeed a great reduction in grey matter thickness, an increase of tissue damage-related markers in region functionally-connected to the olfactory cortex, and an overall brain size reduction were reported as distinctive traits displayed after SARS-CoV-2 infection (Douaud et al., 2022). The presence of pre-existing neurological disorders is associated with an increased risk of developing COVID-19-related neurological signs (Chou et al., 2021). Indeed, it has been demonstrated *in-vivo* and *in-vitro* that SARS-CoV-2 is able to infect different types of neurons with different degrees of success (Valeri et al., 2021; Gugliandolo et al., 2021; Lopez et al., 2022; Zhang et al., 2020; Wang et al., 2021; Pellegrini et al., 2020; Jacob et al., 2020; Song et al., 2021; Ramani et al., 2020a). It was suggested that SARS-CoV-2 might use the dopamine receptor as an additional entry receptor (Khalefah and Khalifah, 2020). More generally, in light of the COVID-19-related symptomatology, it has been hypothesized that SARS-CoV-2 might affect the dopamine production (Brundin et al., 2020; Attademo and Bernardini, 2021; Nataf, 2020; Shuibing et al., 2021; Smeyne et al., 2022; Bauer et al., 2022a). However, concerning this issue, no scientific evidence has been produced so far.

From this scenario, our research stems out. We exploited an *in-vitro* model represented by human iPSC differentiated to dopaminergic neurons (DA neurons) infected with three SARS-CoV-2 variants (EU, Delta, Omicron). Together with an intense production neuronal stress markers, neurons present alterations in the expression of both mRNA and proteins involved in the dopamine metabolism. Overall, SARS-CoV-2 infection resulted in a decrease of dopamine production at different degrees, based on the viral variant employed.

2. Material and methods

2.1. iPSC culture

Human iPSC clonal line obtained from primary fibroblasts of a healthy subject was purchased from Coriell Institute (AICS-0022-037). Parental hiPSC line (WTC/AICS-0 at passage 33) derived from fibroblasts was reprogrammed using episomal vectors (OCT3/4, shp53, SOX2, KLF4, LMYC, and LIN28). iPSCs were grown in geltrex-coated (1% for 1 h at 37 °C) 6-well plates and cultured in complete Essential 8 Medium. At 80–90% confluence, cells were passaged using Accutase (3 min 37 °C) and plated at a density of 10^4 cells/cm^2 in complete Essential 8 Medium supplemented with 10 μM Rock inhibitor for 24 h.

2.2. Differentiation of iPSC to dopaminergic neurons

iPSCs were differentiated to DA neurons according to the protocol described by Zhang et al. (Zhang et al., 2014). Cells at 70% confluence were cultured in proper media as follows:

- day 0: KSR medium (81% DMEM, 15% KSR, 100 × 1% non-essential amino acids, 100 × 1% 2-mercaptoethanol, 100 U/ml penicillin, and 100 μg/ml streptomycin) supplemented with 10 μM SB431542 and 100 μM LDN-193189;
- days 1 and 2: KSR medium supplemented with 10 μM SB431542, 100 nM LDN-193189, 0.25 μM SAG, 2 μM purmorphamine, and 50 ng/mL FGF8b;
- days 3 and 4: KSR medium supplemented with 10 μM SB431542, 100 nM LDN-193189, 0.25 μM SAG, 2 μM purmorphamine, 50 ng/mL FGF8b, and 3 μM CHIR99021;
- days 5 and 6: 75% KSR medium and 25% N2 medium (97% DMEM, 100 × 1% N2 supplement, 100 U/ml penicillin, and 100 μg/ml streptomycin) supplemented with 100 nM LDN-193189, 0.25 μM SAG, 2 μM purmorphamine, 50 ng/mL FGF8b, and 3 μM CHIR99021;
- days 7 and 8: 50% KSR medium and 50% N2 medium supplemented with 100 nM LDN-193189 and 3 μM CHIR99021;
- days 9 and 10: 25% KSR medium and 75% N2 medium supplemented with 100 nM LDN-193189 and 3 μM CHIR99021;
- days 11 and 12: B27 medium (95% Neurobasal medium, 50 × 2% B27 supplement, 1% Glutamax, 100×, 100 U/ml penicillin, and 100 μg/ml streptomycin) supplemented with 3 μM CHIR99021, 10 ng/mL BDNF, 10 ng/mL GDNF, 1 ng/mL TGF-b3, 0.2 mM ascorbic acid, and 0.1 mM cyclic AMP;
- from day 13 to the end of differentiation: B27 medium supplemented with 10 ng/mL BDNF,10 ng/mL GDNF, 1 ng/mL TGF-β3, 0.2 mM ascorbic acid, and 0.1 mM cyclic AMP.

After 20 days of differentiation, cells were split using Accutase (3 min 37 °C) and plated on geltrex- coated plates at a density of 2×10^5 cells/cm^2. At day 26 of differentiation cells were plated at a density of 6×10^4 cells/cm^2 in 12 wells plates and at day 30 of differentiation experiments were performed.

2.3. SARS-CoV-2 infection

The European (EU - B.1), the Delta (B.617.2) and the Omicron (BA.1) SARS-CoV-2 lineages were a kind gift of Dr. Davide Mileto, Clinical Microbiology, Virology and Bio-emergence Diagnosis, ASST Fatebenefratelli-Sacco, Department of Biomedical and Clinical Sciences, University of Milan, Milan, Italy. Viruses were isolated from positive nasopharyngeal swabs, propagated, and titrated using the permissive cell line Vero E6 (ATCC, VA, USA). All SARS-CoV-2 strains were identified by means of whole genome sequencing and the sequences were submitted to GISAID (EU EPI_ISL_41297], Delta EPI_ISL_1970729, and Omicron EPI_ISL_1649798). All the experiments with SARS-CoV-2 virus were performed in BSL3 facility; virus was inactivated according to institutional safety guidelines, before samples analyses outside BSL3 area.

In order to assess infectious viral particles concentration, $TCID_{50}$, was performed as elsewhere described (Fenizia et al., 2022). Briefly, Vero E6 were seeded at 2×10^4 cells per well in a 96-well plate. Eleven 1:10, or 1:3 when needed, serial dilutions of the viral stock were performed in 2% FBS medium. For each dilution, eight wells were infected ($n = 8$). Eight wells were left uninfected as control. 1 -h post infection (hpi), each well was thoroughly washed three times with pre-warmed PBS and the culture media replaced with 10% FBS DMEM. At 72 hpi, supernatants were removed, cells fixed by paraformaldehyde (PFA - Sigma-Aldrich, MO, USA) 4% for 1 h at room temperature, then stained by 0.2% crystal violet solution (Sigma-Aldrich, MO, USA). By applying the Reed-Muench method with the correction for the proportional distance (PD) (Reed and Muench, 1938), we were able to assess the $TCID_{50}$ and to calculate the MOI in our experiments.

Then, DA neurons were challenged with 5, 0.5 or 0.05 MOI of SARS-CoV-2. After an over-night incubation, cells were thoroughly washed three times with pre-warmed PBS and replenished with the complete growth medium. Upon media refill, at 0, 48 and 96 hpi, supernatants were collected to monitor infection. At 48, 72 and 96 hpi, cells were lysed for RNA or protein extraction, whereas supernatants were harvested and appropriately stored.

2.4. Other stimuli

DA neurons were challenged with 1 μg/ml LPS, with 5 MOI of respiratory syncytial virus (RSV) or with 5 MOI of heat-inactivated EU SARS-CoV-2 (iSARS). iSARS was obtained by heating the virus for 20′ at 70 °C (Batéjat et al., 2021).

2.5. MTT

Cytotoxic effect was evaluated by means of an MTT assay: cells were

seeded in 96-well plates (2×10^4 per well) infected with SARS-CoV-2 viruses at different concentrations (from 10^2 MOI down to 10^{-8} MOI, applying serial 10^1 dilution; $n = 8$) or mock infected (CTRL). At 96 hpi, cell viability was assessed by 3-(4,5-dimethylthiazol-2-yl)-2,5-diphenyltetrazolium bromide (MTT) method. Briefly, 30 µl of MTT (final concentration, 0.5 mg/mL) was added to each well under sterile conditions, and the 96-well plates were incubated for 4 h at 37 °C. Supernatants were removed, and dimethyl sulfoxide (100 µl/well) was added. The plates were then agitated on a plate shaker for 5 min. The absorbance of each well was measured at 490 nm with a Bio-Rad automated EIA analyzer (Bio-Rad Laboratories, Hercules, CA, USA). The viability of CTRL cells was considered 100%, while the other conditions were expressed as percentages of CTRL.

2.6. mRNA extraction and quantification

Culture supernatants were collected, and Maxwell RSC Viral Total Nucleic Acid purification kit was used to extract RNA from 250 µl of cell culture supernatants employing the Maxwell RSC Instrument (Promega, WI, USA). Each well was then thoroughly washed three times with pre-warmed PBS. Cells were lysed and collected in 100 µl of RNAzol (TEL-TEST Inc., TX, USA). RNA extraction was performed employing the acid guanidium-phenol-chloroform (AGPC) extraction method, as elsewhere described (Fenizia et al., 2021). Finally, RNA was reverse-transcribed and amplified by OneStep MMix (Promega, WI, USA) on a CFX Opus real-time thermocycler (Bio-rad, CA, USA). cDNA quantification for IFITM1 (– F 5'-TCTTGAACTGGTGCTGTCTGG-3′; R 5'-ACTTGGCGGTGGAGGCATAG-3′), IFITM3 (F 5'-ACTGGGATGACGATGAGCA-3′; R 5'-AGCATTCGCCTACTCCGTGA-3′), MxA (F 5'-CCAGAGGCAGGAGACAATCAG-3′; R 5'-TCTTCGGTGGAACACGAGGT-3′), TH (F 5'-CGACCCTGACCTGGACTTGGA-3′; R 5'-GGCAATCTCCTCGGCGGTGT-3′), VMAT2 (F 5'-CCATTGCGGATGTGGCATTT-3′; R 5'-TCTTCTTTGGCAGGTGGACTT-3′) (Sigma Aldrich, MI, USA), S100B (Assay ID: qHsaCED0045890), DDC (Assay ID: qHsaCED0037636), DAT (Assay ID: qHsaCID0006207) (Bio-rad, CA, USA), SARS-CoV-2 N1 (F 5'-CAATGCTGCAATCGTGCTAC-3′; R 5'-GTTGCGACTACGTGARGAGG-3′) and N2 (F 5'-GCTGCAACTGTGCTACAACT-3′; R 5' TGAACTGTTGCGACTACGTG-3′) (IDT, IA USA) was analyzed as ΔΔCt and presented as relative ratio between the target gene and the GAPDH housekeeping mRNA.

2.7. Protein determination

Protein concentration of samples was assessed with the DC™ protein assay kit according to manufacturer's instructions, using bovine serum albumin at different concentrations as standard.

2.8. Immunoblotting

Immunoblotting for DA neurons total cell lysates were performed using standard protocols. Aliquots of proteins were mixed with Laemmli buffer (0.15 M DTT, 94 mM Tris-HCl pH 6.8, 15% glycerol, 3% *w/v* SDS, 0.015% blue bromophenol) and heated for 5 min at 95 °C. Proteins were separated on 4–20% polyacrylamide gradient gels and transferred to PVDF membranes by electroblotting. PVDF membranes were incubated in blocking solution (5% non-fat dry milk (*w/v*) in TBS-0.1% tween-20 (*v/v*)) at 23 °C for 1 h under gentle shaking. Subsequently, PVDF membranes were incubated overnight at 4 °C with primary antibodies diluted in blocking solution. The day after, PVDF membranes were incubated for 1 h at 23 °C with secondary HRP-conjugated antibodies diluted in blocking solution. PVDF were scanned using the chemiluminescence system Alliance Mini HD9 (Uvitec, Cambridge, United Kingdom) and band intensity was quantified using ImageJ software (v2.1.0/1.53c). The following primary antibodies were used for immunoblotting: monoclonal mouse anti-TH (dilution: 1:2500; RRID: AB_628422), polyclonal rabbit anti-MAP2 (dilution: 1:1000; RRID: AB_10693782), monoclonal mouse anti-Tau (dilution: 1:1000; RRID: AB_10695394), polyclonal rabbit anti-GAPDH (dilution: 1:10000; RRID: AB_796208), monoclonal mouse anti-calnexin (dilution:1:1000; RRID: AB_397884). The following secondary antibodies were used: Goat-anti-rabbit HRP-conjugated (1: 2 000; RRID: AB_2099233) and Goat-anti-mouse HRP conjugated (dilution: 1: 2 000; RRID: AB_228307).

2.9. Immunocytochemistry

Cells were seeded on coverslips in a 24-well. 48 h post infection assay, SARS-CoV-2 infected and not infected cells were fixed in PBS containing 4% paraformaldehyde (PFA) at RT for 10 min, followed by permeabilization with 0,1% TritonX-100 in PBS for 10 min. Cells were treated with PBS 1% BSA for blocking at RT for 1 h, and incubated with primary antibodies: anti-N Nucleocapsid SARS-CoV-2 antibody (cell signalling, #33717), 1:400; MAP2 (cell signalling, #4542), 1:1000; GLUK2 (abcam, ab66440), 1:200; Pax6 (DSHB, AB_528427), 1:250; Sox2 (Millipore, AB5603), 1:500; TH (R&D, MAB7566), 1:100; Nestin (Cell signalling, #33475), 1:100; GABA (Sigma, A2129), 1:500, at 4 °C o.n. and stained with secondary antibodies (Alexa Fluor 488, 586 or 647, 1:500, abcam, Cambridge, UK) for 1 h at RT. Coverslips were mounted using a mounting medium with DAPI (Enzo Life Sciences, Milan, Italy). Confocal imaging was performed with a Leica TCS SP8 System equipped with a DMi8 inverted microscope and a HC PL AP0 40×/1.30 Oil CS2 (Leica Microsystems, Wetzlar, Germany) at a resolution of 1024 × 1024 pixels.

2.10. Dopamine measurement

Total dopamine levels in the cell lysates and in the culture medium were quantified using a direct competitive chemiluminescent enzyme-linked immunosorbent assay (ELISA) dopamine kit (Catalog number: EU0392, Fine Test®, Wuhan, China) according to the manufacturer's instructions. Absolute values were obtained based on a standard curve and expressed as ng of dopamine/ ml/ mg proteins.

2.11. Statistical analyses, graphs and images

For the study variables, medians and ranges were reported for quantitative variables. *t*-test and ANOVA were used with a p value threshold of 0.05. The analyses were performed using GraphPad Prism 8. Graphs and images were assembled by GraphPad Prism 8 and Biorender.com, respectively.

All experiments were confirmed in 3 independent replicates ($n = 3$) and all the procedures were carried out in accordance with the GLP guidelines adopted in our laboratories.

3. Results

3.1. SARS-CoV-2 infection of dopaminergic neurons

First, we proceeded with the characterization of the dopaminergic neurons in culture (Fig. 1). As depicted, we obtained 100% of dopaminergic (DA) neurons, according to the TH and MAP2 staining.

In addition, as shown in Fig. S1 these neurons present a low expression of SOX2 pluripotency marker and of the neuronal precursor markers PAX6 and Nestin. We found a scant staining of GLUK2 and GABA, suggesting a minor glutamatergic and GABAergic commitment.

Then, we exposed the DA neurons to different concentrations of EU SARS-CoV-2, ranging from 5×10^2 to 5×10^{-8} MOI. At 96 hpi we detected no significant changes in cell viability compared to the uninfected control, by the means of an MTT assay (Fig. 2A). Similar results were obtained for Delta or Omicron SARS-CoV-2 variants (Fig. S2).

Overtime, we could detect by real-time PCR a modest but steady increase of SARS-CoV-2 N1 and N2 RNA in DA neurons exposed to 5 MOI of SARS-CoV-2 (EU, Delta or Omicron) (Fig. 2B). The SARS-CoV-2

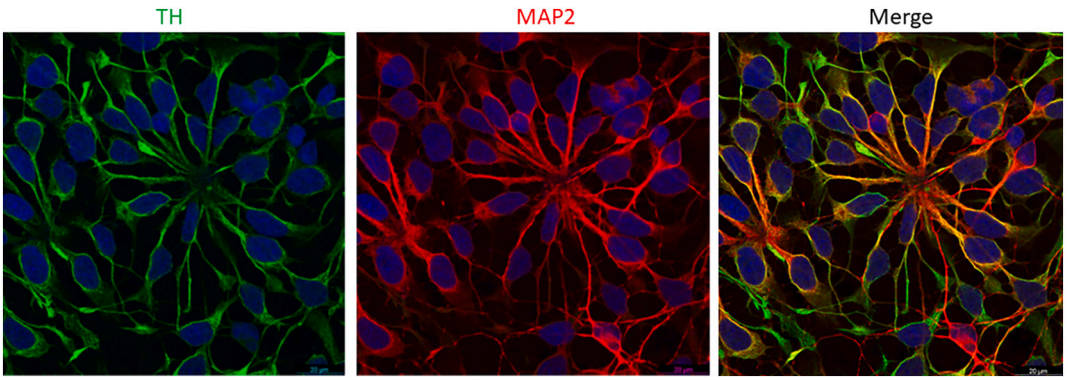

Fig. 1. Human iPSC-derived dopaminergic neurons. ICC of DA neurons at day 30 of culture. Cells were stained for TH (green) and MAP2 (red). Nuclei were stained in blue. Images were acquired with a 40× magnification. (For interpretation of the references to colour in this figure legend, the reader is referred to the web version of this article.)

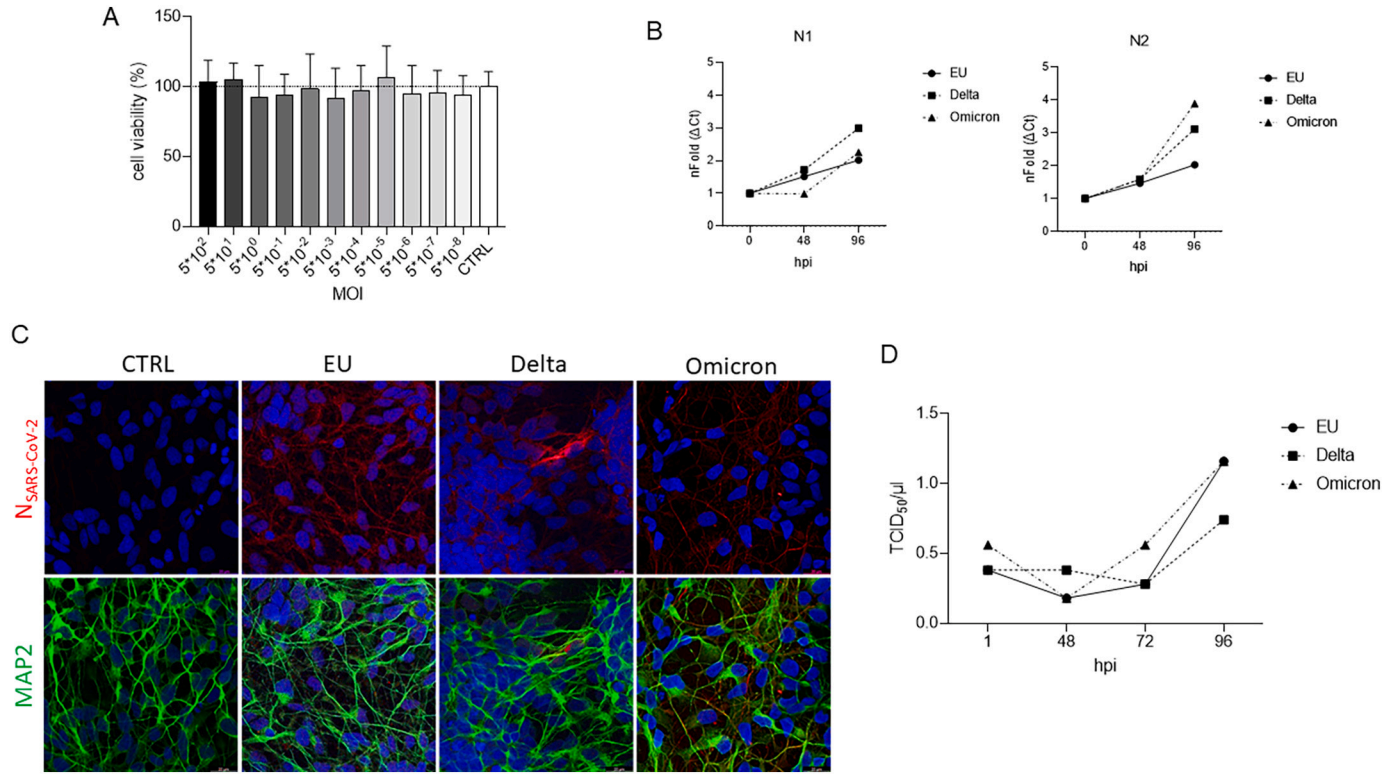

Fig. 2. *In vitro* SARS-CoV-2 infection of human iPSC-derived dopaminergic neurons. Panel A) MTT viability assay at 96 hpi with EU SARS-CoV-2. Viral concentrations range from $5*10^{2}$ to $5*10^{-8}$ on a 1:10 dilution basis. Data are shown as percentage of the uninfected control. Panel B) Upon *in vitro* challenge of DA neurons with 5 MOI of SARS-CoV-2 (EU, Delta or Omicron), the infection was monitored at 0, 48 and 96 hpi. Real-time PCR for N1 (left, Anova time factor $p \leq 0.02$) and N2 (right, Anova time factor $p \leq 0.02$) viral genes was performed. Results are shown as nFold (ΔCt). Panel C) ICC of DA neurons at 96 hpi with 5 MOI of EU, Delta or Omicron SARS-CoV-2 variants, or mock infected (DAPI in blue, NSARS-CoV-2 in red, MAP2 in green). Panel D) Titration of progeny SARS-CoV-2 virus (EU, Delta or Omicron variants) in the DA neurons culture supernatant harvested at 0, 48, 72 and 96 hpi. Data are shown as $TCID_{50}$/µl (Anova time factor $p \leq 0.005$). (For interpretation of the references to colour in this figure legend, the reader is referred to the web version of this article.)

infection in DA neurons was confirmed by immunocytochemistry (ICC) at 96 hpi, by detecting the viral protein N at the intracellular level (Fig. 2C). We observed sporadic N2 positive DA neurons upon infection with 0.5 MOI as well (Fig. S3).

In order to test whether the progeny virus could be infectious, we collected the supernatants of the infected DA neurons throughout the 96-h culture. Such supernatants were then tested by $TCID_{50}$ assay on VeroE6 cells (Fig. 2D). Results show a modest infectious ability of the progeny virus for all the three SARS-CoV-2 variants considered, EU, Delta and Omicron, reaching at 96 hpi 1.16, 0.74 and 1.16 $TCID_{50}$/µl, respectively.

3.2. Neuronal stress markers

DA neurons infected with 5 MOI of SARS-CoV-2 (EU) were assessed for innate immunity or stress markers 48, 72, 96 hpi. By real-time PCR, we measured the mRNA expression of different virus-specific intracellular response genes (IFITM1, IFITM3 and MxA) and a neuronal stress-related marker (S100B) (Fig. 3A). While IFITM1 was not regulated by SARS-CoV-2 infection, we observed IFITM3, MxA and S100B to be upregulated over time ($p = 0.0139$, $p = 0.0002$, $p < 0.0001$) reaching a significant increase at 96 hpi. Therefore, we tested also the effect of Delta and Omicron variants in these very same conditions. As shown in

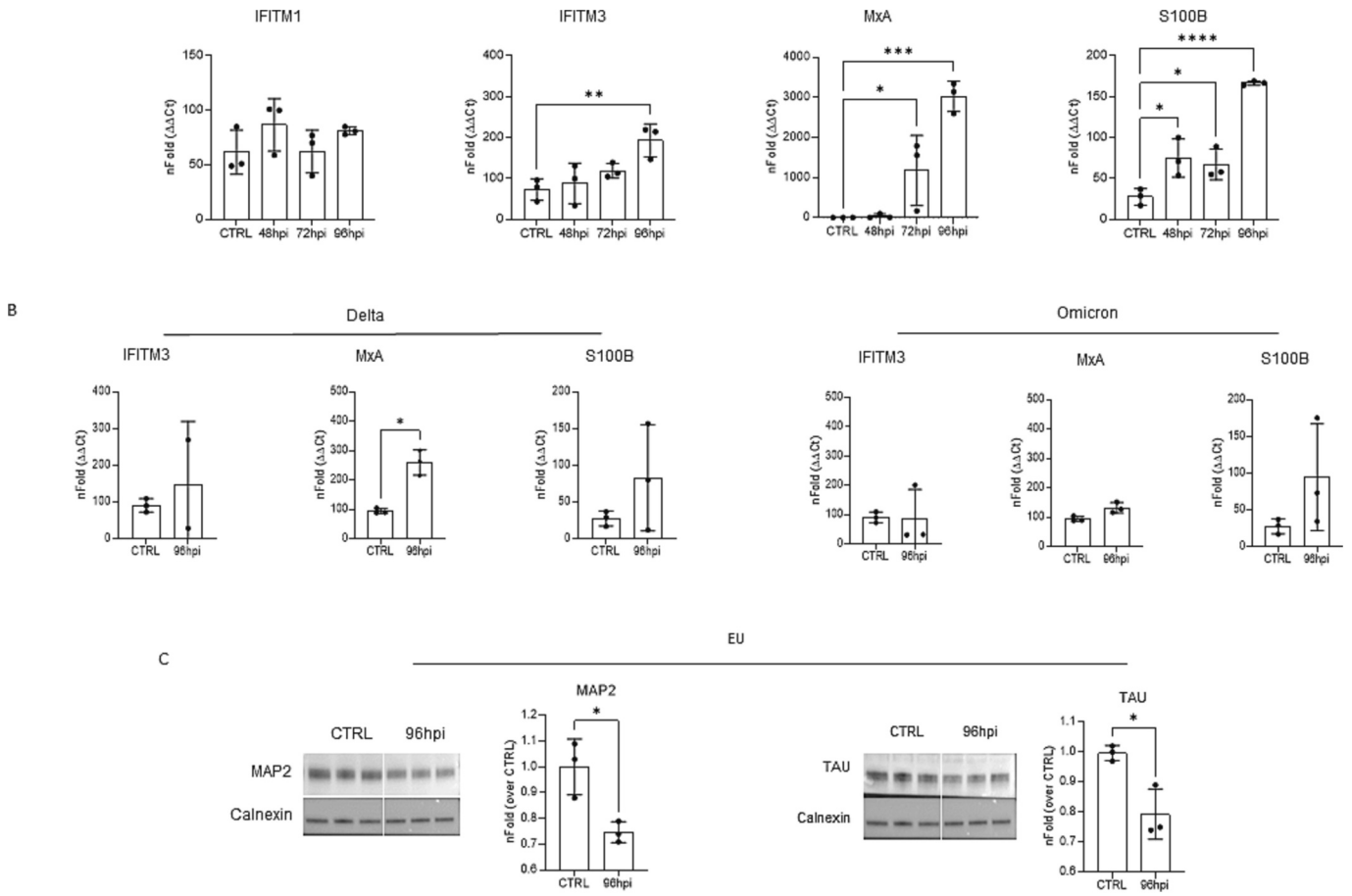

Fig. 3. Effect of SARS-CoV-2 variants on antiviral and neuronal stress markers. Panel A) Real-time PCR expression analyses, expressed as nFold (ΔΔCt), of the antiviral innate neuronal immune response markers MxA, IFITM1 and IFITM3 and the neuronal stress marker S100B, triggered by the EU SARS-CoV-2 variant at 48, 72 and 96 h post infection (hpi). Panel B) Real-time PCR expression analyses of MxA, IFITM3 and S100B triggered by the Delta (left) and Omicron (right) SARS-CoV-2 variant at 96 hpi. Panel C) Western blot analyses of the neuronal marker MAP2 and TAU in DA neurons infected by the EU SARS-CoV-2 variant at 96 hpi. Band intensity of each antigen was normalized over calnexin and expressed as fold change over the control. Statistical significance was calculated by multiple comparison test or by Student's *t*-test, where appropriate. * ≤0.05; ** ≤0.01; *** ≤0.005; **** ≤0.0001 ($n = 3$).

Fig. 3B the only observed effect was an upregulated expression for MxA upon infection of DA neurons with the Delta variant.

By immunoblotting analyses, the expression of MAP2 and Tau protein was evaluated in SARS-CoV-2 infected cells at 96 hpi. Both of them were found to be decreased by EU- SARS-CoV-2 infection ($p = 0.0191$ and $p = 0.0158$, respectively) (Fig. 3C), but not by Delta or Omicron-SARS-CoV-2 infection (Fig. S4 A and B, respectively). The data was supported also by immunocytochemistry against MAP2, which showed a fragmented staining in neurons infected by EU- SARS-CoV-2 (Fig. S5).

These data suggest that at 96 hpi with SARS-CoV-2- EU dopaminergic neurons undergo neuronal stress.

3.3. Dopamine metabolic pathway

Considering the symptomatology manifested by COVID-19 patients, which seems to involve the dopaminergic tone, we focused our attention on the dopamine metabolic pathway.

First, we measured by ELISA the intracellular dopamine content (Fig. 4A) and the amount secreted in the extracellular environment (Fig. 4B). In addition, we evaluated if the SARS-CoV-2 effect on dopamine production might be virus-dose or variant dependent. In order to do so, we challenged DA neurons with 0.05, 0.5 or 5 MOI of SARS-CoV-2 EU, Delta, or Omicron variants. Results at 96 hpi show that both the EU and the Delta SARS-CoV-2 variants were able to hamper the dopamine production and secretion, while no significant effect was detected in Omicron-infected neurons.

In particular, for the EU and Delta SARS-CoV-2 variant the dopamine content inversely correlates with the MOI of virus employed (Anova $p \leq 0.02$ and $p \leq 0.01$, respectively). On the other hand, the reduction in dopamine secretion for the EU- SARS-CoV-2 variant was not virus-dose dependent, whereas for the Delta- SARS-CoV-2 variant (Anova $p \leq 0.001$), we observed a decrease of about 30% only upon the infection with 5 or 0.5 MOI. To better investigate this aspect, 96 hpi we evaluated the protein expression and the mRNA levels of the main players involved in dopamine metabolism (Fig. 5).

The protein levels of tyrosine hydroxylase (TH), the enzyme that converts tyrosine to DOPA, resulted strongly reduced upon infection with both EU and Delta variants ($p \leq 0.05$ and $p \leq 0.005$, respectively) (Fig. 5A). Conversely, in DA neurons, the mRNA expression of TH was significantly upregulated ($p < 0.0001$) only upon infection with 5 MOI of SARS-CoV-2- EU and Delta (Fig. 5B). Moreover, the infection with EU and Delta variants determined the downregulation in the mRNA expression of two key molecules of dopamine metabolism, the DOPA decarboxylase (DDC; $p \leq 0.05$) and the dopamine transporter (DAT; $p \leq 0.05$) (Fig. 5B). In addition, the mRNA level of the vesicular monoamine transporter 2 (VMAT2) displayed a modest increase only upon SARS-CoV-2- EU infection (Fig. 5B). Any change was observed upon infection with Omicron SARS-CoV-2 (Fig. 5B).

To further assess whether the effect of SARS-CoV-2 on DA neurons was virus-specific or generally stress-related, we challenged these cells with other stimuli, such as LPS, the respiratory syncytial virus (RSV), or the heat-inactivated EU SARS-CoV-2 (iSARS). Any of these stimuli is

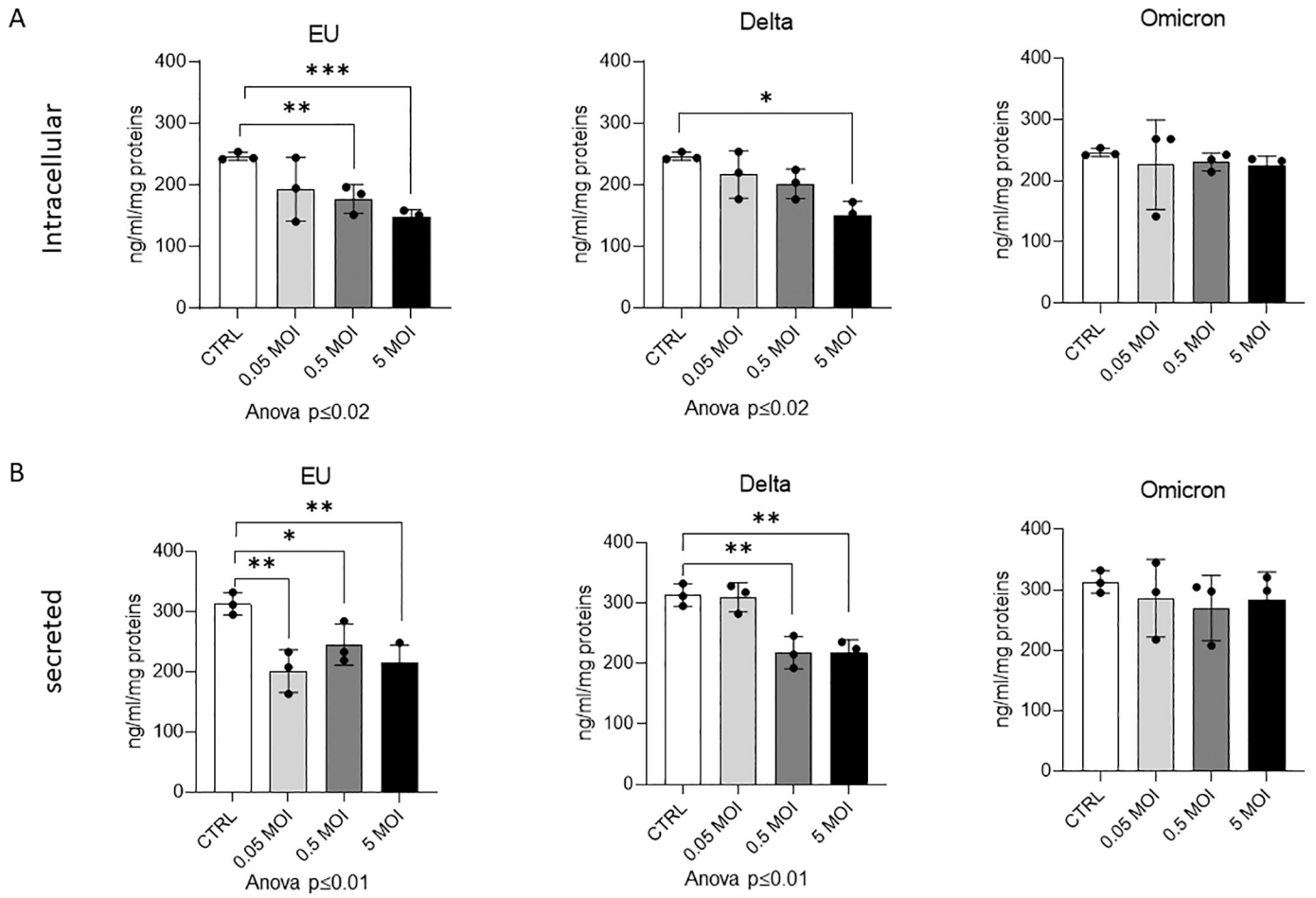

Fig. 4. Effect of SARS-CoV-2 variants on dopamine production. Panel A) Intracellular dopamine quantification by ELISA upon challenge with 0.05 MOI, 0.5 MOI, and 5 MOI of EU (Anova $p \leq 0.02$) (left), Delta (middle) (Anova $p \leq 0.02$), and Omicron (right) SARS-CoV-2 variants, or the uninfected control, at 96 hpi. Panel B) Secreted dopamine quantification by ELISA upon challenge with 0.05 MOI, 0.5 MOI, and 5 MOI of EU (left), Delta (middle) (Anova $p \leq 0.001$), and Omicron (right) SARS-CoV-2 variants, or the uninfected control, at 96 hpi. The depicted statistical significance is relative to multiple comparison t-test only. * ≤0.05; ** ≤0.01; *** ≤0.005 (n = 3).

able to significantly modulate the antiviral response (Fig. 6A) or to affect the dopamine metabolism (Fig. 6B-C).

4. Discussion

The neurotropic effect of viruses represents an important item of virology, since the infection of an immune privileged site as the brain could have both short and long- term severe consequences, due to the post- mitotic stage of neurons. Although several viruses are reported to infect neurons, scant is the information related to the family Coronaviridae. Retrospective analyses on patients infected by H1N1 virus during the influenza pandemic of 1918, report an increased prevalence of lethargic encephalitis associated with Parkinsonism (Dourmashkin, 1997; Reid et al., 2001). Arboviruses are known to affect neurons and to dampen catecholamine biosynthesis (Elizan et al., 1978; Clarke et al., 2014; Mpekoulis et al., 2022), while Herpes simplex virus specifically targets the TH (Rubenstein et al., 1985; Price et al., 1981).

Emerging evidence supports also the effect of SARS-CoV-2 infection on both CNS and PNS. In particular, a large fraction of patients experiences symptoms such as post exertional malaise, brain fog, neurological sensations, headaches, memory issues, insomnia, muscles aches, dizziness/ balance issues, speech issues, joint pain, sleep disturbance, anxiety and depression (Davis et al., 2021; Huang et al., 2021; Tomasoni et al., 2021). In addition, a broad spectrum of signs affecting the dopaminergic tone has been described among patients affected by COVID-19.

Currently, the extent of SARS-CoV-2 infection in the brain is not well defined in humans. Despite this clinical evidence, poor is the information related to the effect of SARS-CoV-2 infection on neuronal homeostasis. In a recent paper published by Pedrosa et al. it has been demonstrated that the EU variant of SARS-CoV-2 presented a limited capability to infect neurons, whereas it showed an infectivity for astrocytes, which, by the induction of an inflammatory response, lead indirectly to neuronal damage (da SG et al., 2021). The SARS-CoV-2 tropism for astrocytes, together with the consequent inflammatory response and cell dysfunction, was confirmed by multiple authors (Andrews et al., 2022; Kong et al., 2022). Some of these observations were recapitulated in a mouse model, reporting an increased susceptibility to oxidative stress in DA neurons from infected mice (Smeyne et al., 2022). However, the authors did not test for the actual infection of those neurons. Although Spike-bearing pseudoviruses corroborate the hypothesis of a direct infection of DA neurons (Yang et al., 2020), the SARS-CoV-2 infection of such neurons remains somehow elusive, so far. In our work we tried to address this issue exploiting the use of human DA neurons derived from iPSCs. Our differentiation protocol allows to obtain a neuronal population entirely expressing the dopaminergic marker TH. As usually occurs for iPSCs differentiation we observed also a scant expression of the neuronal precursor markers Nestin and PAX6. Nevertheless, compared to the neuronal marker MAP2 and TH, the expression level of these precursor markers is very low suggesting a late stage of maturation of DA neurons. Using this model, we found that the

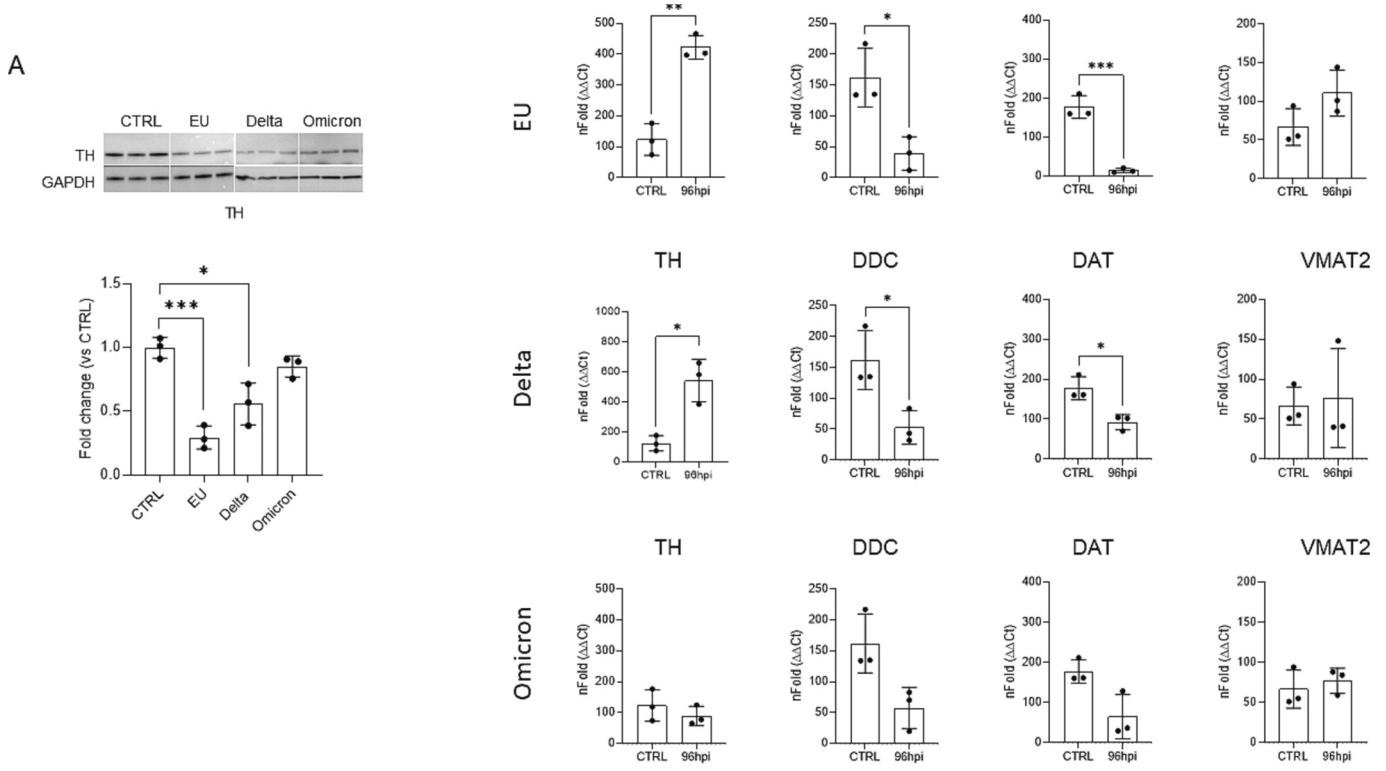

Fig. 5. Effect of SARS-CoV-2 variants on the dopamine biosynthetic pathway. Panel A) Western blot analyses of TH upon challenge with EU, Delta and Omicron SARS-CoV-2 variants at 96 hpi. Band intensity of each antigen was normalized over GAPDH and expressed as fold change over the control (Anova $p \leq 0.0002$). Panel B) Real-time PCR expression analyses, expressed as nFold (ΔΔCt), of the tyrosine hydroxylase (TH), the DOPA decarboxylase (DDC), the dopamine transporter (DAT) and the vesicular monoamine transporter 2 (VMAT2) mRNA, upon challenge with the EU (top), Delta (middle) and Omicron (bottom) SARS-CoV-2 variant at 96 hpi. Statistical significance was calculated by Student's t-test. * ≤0.05; ** ≤0.01; *** ≤0.005 (n = 3).

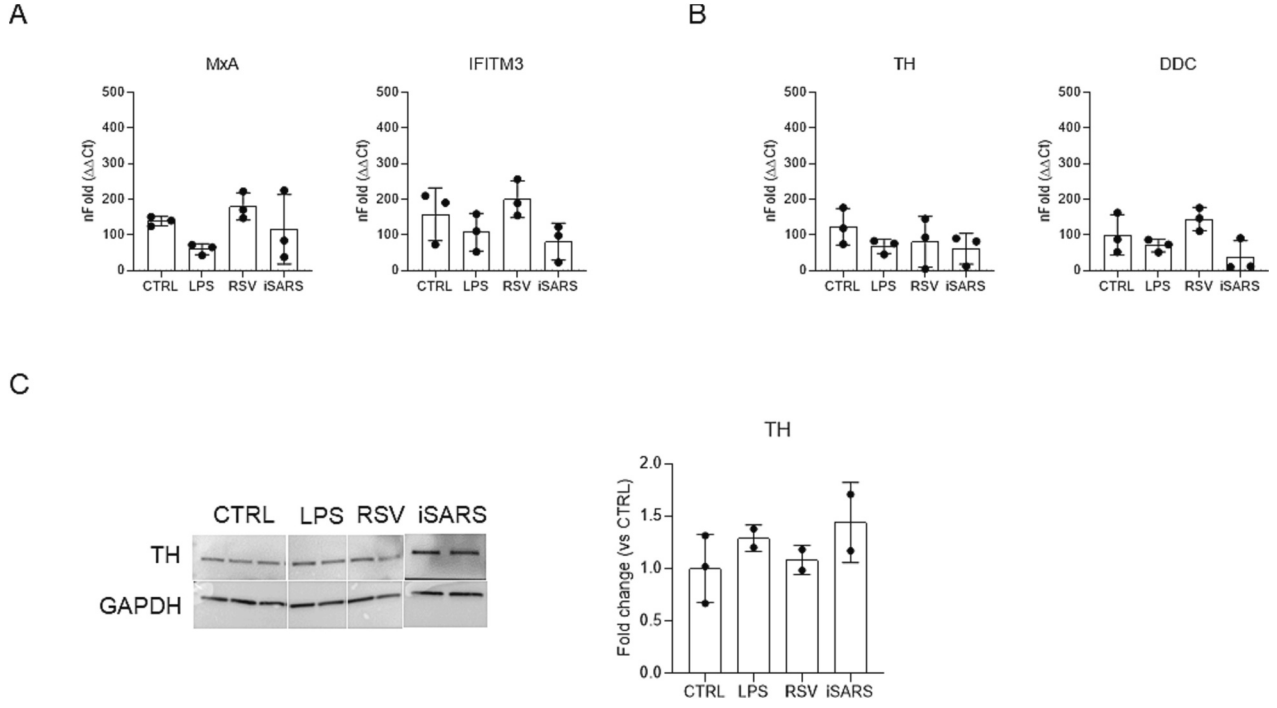

Fig. 6. Effect of other stimuli on the antiviral response and the dopamine pathway. Panel A and B) Real-time PCR expression analyses, expressed as nFold (ΔΔCt), of MxA, IFITM3, TH and DDC upon challenge of DA neurons with LPS, RSV and heat-inactivated SARS-CoV-2 (iSARS). Panel C) Western blot analyses of TH upon challenge of DA neurons with LPS, RSV and iSARS. Band intensity of each antigen was normalized over GAPDH and expressed as fold change over the control. Statistical significance was calculated by Student's t-test. (n = 3).

EU, Delta, and Omicron SARS-CoV-2 variants showed a low productive infection in DA neurons, even if administered at high MOI. Interestingly, we observed that the infection with EU and Delta SARS-CoV-2 promotes the neuronal innate immune response as demonstrated by the increased mRNA expression of MxA and IFITM3 (Feeley et al., 2011; Zhao et al., 2014; Spence et al., 2019; Verhelst et al., 2013; Sadler and Williams, 2008). Such genes are enclosed in the so-called interferon response and are known to be key players in the intracellular antiviral response, which can rely on different finely- tuned pathways. Indeed, in our model, IFITM3 and MxA were upregulated, while IFITM1 was not, underlying the specificity of the antiviral response triggered by SARS-CoV-2 in DA neurons. In addition, EU infection caused also the upregulation of the neuronal stress marker S100B, which was previously related to SARS-CoV-2 disease severity and neuronal damage (Ramani et al., 2020b; Aceti et al., 2020; Tremblay et al., 2020). These data clearly indicate that the infection with different variants of SARS-CoV-2 affects the homeostasis of DA neurons. Since DA neurons are the main actors for the production of dopamine in brain, we investigated whether the SARS-CoV-2 infection affects this pathway. A proof that SARS-CoV-2 infection could affect the dopamine metabolism derives also from a recent paper by Mpekoulis G. et al. in which it has been described that the infection of non- neuronal cells determines a reduction in the mRNA expression of DDC (Mpekoulis et al., 2021; Limanaqi et al., 2022).

The order of magnitude that SARS-CoV-2 viral load could potentially reach in the human brain *in vivo* is currently unknown. Some hints might come from the observation that SARS-CoV-2 is endowed of a marked tropism for astrocytes (da SG et al., 2021; Andrews et al., 2022). Andrews and colleagues detected a viral load between 10^4 and 10^5 PFU/ml as order of magnitude at 72 hpi in the supernatant of SARS-CoV-2-infected neurospheres, mainly ascribable to astrocytes (Andrews et al., 2022). Comparing this to our experimental setting, it would translate to an order of magnitude of 10^{-1} MOI, which is the intermediate dose among those tested. Overtime, the viral load could easily accumulate even higher. Although this does not prove the point, to our best knowledge, it is suggestive that the amount of SARS-CoV-2 employed in our experiments *in vitro* is likely to be potentially reached *in vivo*.

In our work, by titrating the progeny virus, we demonstrated that SARS-CoV-2 not only infects, but also propagates in DA neurons. Moreover, we demonstrated that SARS-CoV-2 infection of DA neurons is able to impair dopamine metabolism inducing a reduction in the production of dopamine and in its release in the extracellular environment, only upon the infection with the EU and Delta SARS-CoV-2 variants, but not with the Omicron one.

We speculate that these data might relate to the clinical observation that EU or Delta -infected patients manifest the most severe neuronal symptomatology with respect to those infected by Omicron variant (Vaira et al., 2023; Shafer, 2022; Brüssow, 2022; Nealon and Cowling, 2022). Indeed, it is currently unknown if the overall milder simptomathology observed in Omicron infected patients is due to the higher level of immunization of the population, or rather due to a reduced aggressiveness or, in this case, to a reduced neutropism of the Omicron variant. Our results suggest the latter ones and are in line with those obtained on iPS-derived cortical neurons and astrocytes, or humanized mice/hamster models (Bauer et al., 2022b; Seehusen et al., 2022; Natekar et al., 2022).

In addition, the opposite trend shown by TH mRNA and protein levels let to speculate about a compensatory mechanism activated by DA neurons in order to restore the dopamine production in a positive feedback manner.

The observation of a functional deficit in DA neurons after SARS-CoV-2 infection stimulates some speculations on the potential translatability in the clinical setting. It is reasonable to hypothesize that the worsening that patients with Parkinson's disease experience during COVID-19 infection and in the subsequent period, short or long post COVID syndrome, may be associated with this functional deficit. This hypothesis could support a scenario in which Parkinson's disease patients would have a transient worsening of symptoms, and then return to the pre-infection condition once fully recovered (Goerttler et al., 2022).

Further confirmations and insights of this mechanism are necessary in order to consolidate this data and guide clinicians towards an increasingly targeted therapy for Parkinson's disease patients suffering from COVID-19 and for patients suffering from post COVID syndrome.

Supplementary data to this article can be found online at https://doi.org/10.1016/j.yexmp.2023.104874.

Ethics approval

Not applicable.

Authors contribution

MA and *CF* conceived the presented idea. GC, EVC and GL further developed the project with the help of SB and CV. EVC, GL, SB and MA managed the iPSC-derived dopaminergic neurons model and performed the protein analyses. GC, CV and *CF* managed the SARS-CoV-2 infection assays and performed the mRNA analyses. EF, MM and SZ performed immunofluorescence imaging experiments. ABDF helped with the interpretation of the data and with stimulating scientific discussions. GC, EMC, GL, MA and *CF* discussed the data and wrote the manuscript. MC critically reviewed the manuscript. GC, EVC and GL equally contributed to the manuscript. MA and *CF* equally contributed to the manuscript.

Funding

Partially supported by grants from Fondazione Alessandro and Vincenzo Negroni Prati Morosini and Fondazione Romeo and Enrica Invernizzi and by EU funding within the NextGenerationEU-MUR PNRR Extended Partnership initiative on Emerging Infectious Diseases (Project no. PE00000007, INF-ACT).

Declaration of Competing Interest

The authors declare no conflict of interests.

Data availability

Data will be made available on request.

Acknowledgement

We would like to thank Dr. Davide Mileto (Clinical Microbiology, Virology and Bio-emergence Diagnosis, ASST Fatebenefratelli-Sacco, Department of Biomedical and Clinical Sciences, University of Milan, Milan, Italy) for providing the isolated and sequenced SARS-CoV-2 strains employed in the present work. Additionally, we would like to thank Dr. Vittorio Scaravilli (Department of Anesthesia, Critical Care and Emergency, Fondazione IRCCS Ca' Granda-Ospedale Maggiore Policlinico, Milan & Department of Pathophysiology and Transplantation, University of Milan, Milan, Italy) for the stimulating scientific discussions.

References

Aceti, A., Margarucci, L.M., Scaramucci, E., Orsini, M., Salerno, G., Di Sante, G., et al., 2020 Oct. Serum S100B protein as a marker of severity in Covid-19 patients. Sci. Rep. 10 (1), 18665.

Andrews, M.G., Mukhtar, T., Eze, U.C., Simoneau, C.R., Ross, J., Parikshak, N., et al., 2022 Jul 26. Tropism of SARS-CoV-2 for human cortical astrocytes. PNAS. 119 (30), e2122236119.

Attademo, L., Bernardini, F., 2021 Jan. Are dopamine and serotonin involved in COVID-19 pathophysiology? Eur. J. Psychiat. 35 (1), 62–63.

Batéjat, C., Grassin, Q., Manuguerra, J.C., Leclercq, I., 2021 Jun. Heat inactivation of the severe acute respiratory syndrome coronavirus 2. J. Biosaf. Biosecur. 3 (1), 1–3.
Bauer, L., Laksono, B.M., de Vrij, F.M.S., Kushner, S.A., Harschnitz, O., van Riel, D., 2022 May. The neuroinvasiveness, neurotropism, and neurovirulence of SARS-CoV-2. Trends Neurosci. 45 (5), 358–368.
Bauer, L., Rissmann, M., Benavides, F.F.W., Leijten, L., van Run, P., Begeman, L., et al., 2022 Sep 5. In vitro and in vivo differences in neurovirulence between D614G, Delta And Omicron BA.1 SARS-CoV-2 variants. Acta Neuropathol. Commun. 10 (1), 124.
Brundin, P., Nath, A., Beckham, J.D., 2020 Dec. Is COVID-19 a perfect storm for Parkinson's disease? Trends Neurosci. 43 (12), 931–933.
Brüssow, H., 2022 Jul. COVID-19: omicron - the latest, the least virulent, but probably not the last variant of concern of SARS-CoV-2. Microb. Biotechnol. 15 (7), 1927–1939.
Carfì, A., Bernabei, R., Landi, F., 2020 Aug 11. For the Gemelli against COVID-19 post-acute care study group. Persistent symptoms in patients after acute COVID-19. JAMA. 324 (6), 603–605.
CDC. Centers for Disease Control and Prevention, 2020. Healthcare Workers. https://www.cdc.gov/coronavirus/2019-ncov/hcp/clinical-care/post-covid-conditions.html.
CDC. Centers for Disease Control and Prevention, 2022. Post-COVID Conditions. https://www.cdc.gov/coronavirus/2019-ncov/long-term-effects/index.html.
Chou, S.H.Y., Beghi, E., Helbok, R., Moro, E., Sampson, J., Altamirano, V., et al., 2021 May. Global incidence of neurological manifestations among patients hospitalized with COVID-19—a report for the GCS-NeuroCOVID consortium and the ENERGY consortium. JAMA Netw. Open 4 (5), e2112131.
Clarke, P., Leser, J.S., Quick, E.D., Dionne, K.R., Beckham, J.D., Tyler, K.L., 2014 Jan. Death receptor-mediated apoptotic signaling is activated in the brain following infection with West Nile virus in the absence of a peripheral immune response. J. Virol. 88 (2), 1080–1089.
Davis, H.E., Assaf, G.S., McCorkell, L., Wei, H., Low, R.J., Re'em, Y., et al., 2021 Aug. Characterizing long COVID in an international cohort: 7 months of symptoms and their impact. eClinicalMedicine 38, 101019.
Douaud, G., Lee, S., Alfaro-Almagro, F., Arthofer, C., Wang, C., McCarthy, P., et al., 2022 Apr. SARS-CoV-2 is associated with changes in brain structure in UK biobank. Nature. 604 (7907), 697–707.
Dourmashkin, R.R., 1997 Sep. What caused the 1918-30 epidemic of encephalitis lethargica? J. R. Soc. Med. 90 (9), 515–552.
Elizan, T.S., Schwartz, J., Yahr, M.D., Casals, J., 1978 May. Antibodies against arboviruses in Postencephalitic and idiopathic Parkinson's disease. Arch. Neurol. 35 (5), 257–260.
Feeley, E.M., Sims, J.S., John, S.P., Chin, C.R., Pertel, T., Chen, L.M., et al., 2011 Oct. IFITM3 inhibits influenza a virus infection by preventing cytosolic entry. PLoS Pathog. 7 (10), e1002337.
Fenizia, C., Galbiati, S., Vanetti, C., Vago, R., Clerici, M., Tacchetti, C., et al., 2021 Jun 8. SARS-CoV-2 entry: at the crossroads of CD147 and ACE2. Cells. 10 (6), 1434.
Fenizia, C., Galbiati, S., Vanetti, C., Vago, R., Clerici, M., Tacchetti, C., et al., 2022 Feb 23. Cyclosporine a inhibits viral infection and release as well as cytokine production in lung cells by three SARS-CoV-2 variants. Microbiol. Spectr. 10 (1), e0150421.
Goerttler, T., Kwon, E.H., Fleischer, M., Stettner, M., Tönges, L., Klebe, S., 2022 Mar. SARS-CoV-2, COVID-19 and Parkinson's disease-many issues need to be clarified-a critical review. Brain Sci. 12 (4), 456.
Gugliandolo, A., Chiricosta, L., Calcaterra, V., Biasin, M., Cappelletti, G., Carelli, S., et al., 2021 Jul 28. SARS-CoV-2 infected pediatric cerebral cortical neurons: transcriptomic analysis and potential role of toll-like receptors in pathogenesis. Int. J. Mol. Sci. 22 (15), 805.
Huang, C., Huang, L., Wang, Y., Li, X., Ren, L., Gu, X., et al., 2021 Jan 16. 6-month consequences of COVID-19 in patients discharged from hospital: a cohort study. Lancet. 397 (10270), 220–232.
Jacob, F., Pather, S.R., Huang, W.K., Wong, S.Z.H., Zhou, H., Zhang, F., et al., 2020 Dec 3. Human pluripotent stem cell-derived neural cells and brain organoids reveal SARS-CoV-2 neurotropism. Cell Stem Cell 27 (6), 937–950.e9.
Khalefah, M.M., Khalifah, A.M., 2020 Dec. Determining the relationship between SARS-CoV-2 infection, dopamine, and COVID-19 complications. J. Taibah. Univ. Med. Sci. 15 (6), 550–553.
Kong, W., Montano, M., Corley, M.J., Helmy, E., Kobayashi, H., Kinisu, M., et al., 2022 Dec. Neuropilin-1 mediates SARS-CoV-2 infection of astrocytes in brain organoids, inducing inflammation leading to dysfunction and death of neurons. mBio 13 (6) e0230822.
Limanaqi, F., Zecchini, S., Dino, B., Strizzi, S., Cappelletti, G., Utyro, O., et al., 2022 May. Dopamine reduces SARS-CoV-2 replication in vitro through downregulation of D2 receptors and upregulation of type-I interferons. Cells. 11 (10), 1691.
Lopez, G., Tonello, C., Osipova, G., Carsana, L., Biasin, M., Cappelletti, G., et al., 2022 Feb. Olfactory bulb SARS-CoV-2 infection is not paralleled by the presence of virus in other central nervous system areas. Neuropathol. Appl. Neurobiol. 48 (1), e12752.
Mpekoulis, G., Frakolaki, E., Taka, S., Ioannidis, A., Vassiliou, A.G., Kalliampakou, K.I., et al., 2021 Jun. Alteration of L-Dopa decarboxylase expression in SARS-CoV-2 infection and its association with the interferon-inducible ACE2 isoform. PLoS One 16 (6), e0253458.
Mpekoulis, G., Tsopela, V., Chalari, A., Kalliampakou, K.I., Panos, G., Frakolaki, E., et al., 2022 Mar. Dengue virus replication is associated with catecholamine biosynthesis and metabolism in hepatocytes. Viruses. 14 (3), 564.
Nataf, S., 2020 Oct. An alteration of the dopamine synthetic pathway is possibly involved in the pathophysiology of COVID-19. J. Med. Virol. 92 (10), 1743–1744.
Natekar, J.P., Pathak, H., Stone, S., Kumari, P., Sharma, S., Auroni, T.T., et al., 2022 May. Differential pathogenesis of SARS-CoV-2 variants of concern in human ACE2-expressing mice. Viruses. 14 (6), 1139.
Nealon, J., Cowling, B.J., 2022 Jan. Omicron severity: milder but not mild. Lancet. 399 (10323), 412–413.
Pellegrini, L., Albecka, A., Mallery, D.L., Kellner, M.J., Paul, D., Carter, A.P., et al., 2020 Dec 3. SARS-CoV-2 infects the brain choroid plexus and disrupts the blood-CSF barrier in human brain organoids. Cell Stem Cell 27 (6), 951–961.e5.
Price, R.W., Rubenstein, R., Joh, T.H., Reis, D.J., 1981 Jun. Tyrosine hydroxylase activity in the superior cervical ganglion during herpes simplex virus infection: correlation with viral titers and viral antigen. Brain Res. 214 (2), 357–370.
Ramani, A., Müller, L., Ostermann, P.N., Gabriel, E., Abida-Islam, P., Müller-Schiffmann, A., et al., 2020 Oct 15. SARS-CoV-2 targets neurons of 3D human brain organoids. EMBO J. 39 (20), e106230.
Ramani, A., Müller, L., Ostermann, P.N., Gabriel, E., Abida-Islam, P., Müller-Schiffmann, A., et al., 2020 Oct 15. SARS-CoV-2 targets neurons of 3D human brain organoids. EMBO J. 39 (20), e106230.
Reed, L.J., Muench, H., 1938 May. A simple method of estimating fifty per cent endpoints. Am. J. Epidemiol. 27 (3), 493–497.
Reid, A.H., McCall, S., Henry, J.M., Taubenberger, J.K., 2001 Jul. Experimenting on the past: the enigma of von Economo's encephalitis lethargica. J. Neuropathol. Exp. Neurol. 60 (7), 663–670.
Rubenstein, R., Price, R.W., Joh, T., 1985. Alteration of tyrosine hydroxylase activity in PC12 cells infected with herpes simplex virus type 1. Arch. Virol. 83 (1–2), 65–82.
Sadler, A.J., Williams, B.R.G., 2008 Jul. Interferon-inducible antiviral effectors. Nat. Rev. Immunol. 8 (7), 559–568.
Seehusen, F., Clark, J.J., Sharma, P., Bentley, E.G., Kirby, A., Subramaniam, K., et al., 2022 May. Neuroinvasion and neurotropism by SARS-CoV-2 variants in the K18-hACE2 mouse. Viruses. 14 (5), 1020.
da SG, Pedrosa C., Goto-Silva, L., Temerozo, J.R., LRQ, Souza, Vitória, G., Ornelas, I.M., et al., 2021 Jul. Non-permissive SARS-CoV-2 infection in human neurospheres. Stem Cell Res. 54, 102436.
Shafer, Steven L., 2022 May 12. Intrinsic severity of the SARS-CoV-2 omicron variant. N. Engl. J. Med. 386 (19), 186.
Shuibing, Chen, Han, Y., Yang, L., Kim, T., Nair, M., Harschnitz, O., et al., 2021 May 21. SARS-CoV-2 infection causes dopaminergic neuron senescence. Res. Sq. rs.3.rs-513461.
Smeyne, R.J., Eells, J.B., Chatterjee, D., Byrne, M., Akula, S.M., Sriramula, S., et al., 2022 Jul. COVID-19 infection enhances susceptibility to oxidative stress–induced parkinsonism. Mov. Disord. 37 (7), 1394–1404.
Song, E., Zhang, C., Israelow, B., Lu-Culligan, A., Prado, A.V., Skriabine, S., et al., 2021 Mar 1. Neuroinvasion of SARS-CoV-2 in human and mouse brain. J. Exp. Med. 218 (3), e20202135.
Soriano, J.B., Murthy, S., Marshall, J.C., Relan, P., Diaz, J.V., 2022 Apr. WHO clinical case definition working group on post-COVID-19 condition. A clinical case definition of post COVID-19 condition by a Delphi consensus. Lancet Infect. Dis. 22 (4), e102–e107.
Spence, J.S., He, R., Hoffmann, H.H., Das, T., Thinon, E., Rice, C.M., et al., 2019 Mar. IFITM3 directly engages and shuttles incoming virus particles to lysosomes. Nat. Chem. Biol. 15 (3), 259–268.
Tomasoni, D., Bai, F., Castoldi, R., Barbanotti, D., Falcinella, C., Mulè, G., et al., 2021 Feb. Anxiety and depression symptoms after virological clearance of COVID-19: a cross-sectional study in Milan, Italy. J. Med. Virol. 93 (2), 1175–1179.
Tremblay, M.E., Madore, C., Bordeleau, M., Tian, L., Verkhratsky, A., 2020 Nov. Neuropathobiology of COVID-19: the role for glia. Front. Cell. Neurosci. 14, 592214.
Vaira, L.A., Lechien, J.R., Deiana, G., Salzano, G., Maglitto, F., Piombino, P., et al., 2023 Feb. Prevalence of olfactory dysfunction in D614G, alpha, delta and omicron waves: a psychophysical case-control study. Rhinology. 61 (1), 32–38.
Valeri, A., Chiricosta, L., Calcaterra, V., Biasin, M., Cappelletti, G., Carelli, S., et al., 2021 Aug 25. Transcriptomic analysis of HCN-2 cells suggests connection among oxidative stress, senescence, and neuron death after SARS-CoV-2 infection. Cells. 10 (9), 2189.
Verhelst, J., Hulpiau, P., Saelens, X., 2013 Dec. Mx proteins: antiviral gatekeepers that restrain the uninvited. Microbiol. Mol. Biol. Rev. 77 (4), 551–566.
Wan, D., Du, T., Hong, W., Chen, L., Que, H., Lu, S., et al., 2021 Nov 23. Neurological complications and infection mechanism of SARS-CoV-2. Signal Transduct. Target. Ther. 6 (1), 406.
Wang, C., Zhang, M., Garcia, G., Tian, E., Cui, Q., Chen, X., et al., 2021 Feb 4. ApoE-isoform-dependent SARS-CoV-2 neurotropism and cellular response. Cell Stem Cell 28 (2), 331–342.e5.
Yang, L., Han, Y., Nilsson-Payant, B.E., Gupta, V., Wang, P., Duan, X., et al., 2020 Jul. A human pluripotent stem cell-based platform to study SARS-CoV-2 tropism and model virus infection in human cells and organoids. Cell Stem Cell 27 (1), 125–136.e7.
Zhang, B.Z., Chu, H., Han, S., Shuai, H., Deng, J., Hu, Y., 2020 Oct. Fan, et al. SARS-CoV-2 infects human neural progenitor cells and brain organoids. Cell Res. 30 (10), 928–931.
Zhang, P., Xia, N., Reijo Pera, R.A., 2014 Sep 15. Directed dopaminergic neuron differentiation from human pluripotent stem cells. J. Vis. Exp. 91, 51737.
Zhao, X., Guo, F., Liu, F., Cuconati, A., Chang, J., Block, T.M., et al., 2014 May. Interferon induction of IFITM proteins promotes infection by human coronavirus OC43. PNAS. 111 (18), 6756–6761.